ENERGY ANALYSIS OF HEAT EXCHANGER IN A HEAT EXCHANGER NETWORK

by

Martina RAUCH [*] ***and Antun GALOVIC***

Faculty of Mechanical Engineering and Naval Architecture, University of Zagreb, Zagreb, Croatia

Original scientific paper
https://doi.org/10.2298/TSCI171231216R

For many years now, heat exchanger optimization has been a field of research for a lot of scientists. Aims of optimization are different, having in mind heat exchanger networks with different temperatures of certain streams. In this paper mathematical model in dimensionless form is developed, describing operation of one heat exchanger in a heat exchanger network, with given overall area, based on the maximum heat-flow rate criterion. Under the presumption of heat exchanger being a part of the heat exchanger network, solution for the given task is resting in a possibility of connecting an additional fluid stream with certain temperature on a certain point of observed heat exchanger area. The connection point of additional fluid stream determines the exchanging areas of both heat exchangers and it needs to allow the maximum exchanged heat-flow rate. This needed heat-flow rate achieves higher value than the heat-flow rate acquired by either of streams. In other words, a criterion for the existence of the maximum heat-flow rate, as a local extremum, is obtained within this mathematical model. Results of the research are presented by the adequate diagrams and are interpreted, with emphasis on the cases which fulfill and those which do not fulfill the given condition for achieving the maximum heat-flow rate.

Key words: *heat exchanger network, energy analysis, dimensionless analysis, maximum heat-flow rate*

Introduction

Heat exchanger networks (HEN) belong to a group of the most important systems in a process industry because they allow more rational energy consumption and significantly enhance efficiency of production facilities [1]. Design of such systems has been and still is one of the most studied fields of process and chemical industry. Methods for design of HEN have advanced: from the graphical method based on pinch analysis [2], through sequential analysis [3], to the simultaneous synthesis [4]. Recent comparison of the main principles [5] has confirmed that simultaneous method shows the best results. But, pinch method has experienced a significant advance in terms of power pinch analysis, used for defining the minimum electric energy consumption [6] or planning [7] and managing [8] carbon gas emissions. Pinch analysis is also used as a part of optimization model for automatic obtaining of the way to capture and contain the carbon as well as exploiting contained carbon gas, in order to satisfy the carbon gas emission limitations [9]. Contemporary technological enhancement of the HEN systems has attracted great attention of the researchers working on improving the energy efficiency of the existing heat transfer systems [10].

* Corresponding author; e-mail: mrauch@fsb.hr

These improvements can be based on pinch technology, as in [11], or on optimization models, as in [12]. On a scale of whole industry, a few input parameters necessary in HEN design vary significantly, like mass-flow rate and stream temperatures in the process. These parameters are often defined as a range of values, not as a single value. Therefore, principle of such systems design should be in accordance with the varying parameters, which will result with the design of flexible systems of HEN [13].

Many publications related to the HEN are based on multi-stream heat exchangers. Saving on capital cost and volume is provided by using multi-stream heat exchanger [14]. Watson *et al*. [15] presented model formulation and solution strategy for design and simulation of processes involving multi-stream heat exchangers in which they combined an extension of pinch analysis with an explicit dependence on the heat exchange area in a non-smooth equation system. During design of multi-stream plate fin heat exchanger, it is important to consider the optimal combination of fin categories and detailed geometries of fin types [16]. For synthesizing large scale multi-stream heat exchanger network (MSHEN) Li *et al*. [17] established a corresponding mathematical model with the objective of minimum total annual cost, and for the optimization the simulated annealing and genetic algorithm is adopted. The multi-period synthesis of MSHEN can be formulated as a mixed integer non-linear programming model and the obtained MSHEN is over-synthesized for all operational period [18]. Yuan *et al*. [19] proposed an approach for synthesizing MSHEN based on the effective temperature levels of streams (stream pseudo temperature). To reduce the search region for the optimal stream match, efficient process stream arrangement strategy is used. Also a stagewise chessboard model expands the new feasible search region as well as avoiding missing optimal matches of other stream arrangements [20].

Many scientific papers dealing with the subject of individual heat exchangers specifically elaborate certain field of heat exchanger application and its performances. Mathematical modeling of heat exchangers using both First and Second law of thermodynamics is usually basic point for further analysis of heat transfer systems. Development of adsorption cooling technique in three aspects is shown in [21]. Mathematical modeling, intrinsic and extrinsic developments are used in order to present review of that field from mathematical modeling to innovative applications. Another mathematical model in [22] is developed for obtaining optimum performance of a double absorption heat transformer. The effects of the operating parameters of heat exchangers and maximum COP and ECOP have been analyzed in detail. Dynamic analysis of lithium bromide-water absorption chiller is given in [23]. Mathematical model has been developed with ability to simulate and predict the behavior of internal and external parameters such as temperature, concentrations, and pressures. An interesting performance analysis of an air-heated humidification-dehumidification desalination plant is given in [24]. Used plate heat exchangers are mathematically modeled and entropy generation of both components and whole system is calculated. Thermodynamics analysis of a combined cooling and power system using ammonia-water mixture is given in [25]. Mathematical models are established to simulate the combined system under steady-state conditions. Exergy destruction analysis is conducted and the results show that the major exergy destruction appears in heat exchangers. Indirect evaporative heat exchanger and a vapor compression system are introduced in [26]. A computational model has been developed to theoretically investigate the performance of indirect evaporative heat exchanger. Taler [27] are mathematically modeling plate fin and tube heat exchanger in order to develop method for numerical modeling of tubular cross-flow heat exchangers. The developed techniques in paper were implemented in digital control system of the water exit temperature in a plate fin and tube heat exchanger. Characteristics of heat pipe heat exchanger used for recovering the waste heat in a slag cooling process in steel industry is given in [28]. Main parameters are investigated experimentally and theoretically and the optimum operation conditions are determined by both First and Second law of thermodynamics.

Examining through the available recent scientific papers from the field of heat exchanger energy analysis it can be stated that concerning papers mainly deal with the analysis on a global scale, while considering only inlet and outlet states of fluid streams. Such approach cannot answer to the demand set within this paper. In this paper the goal of the research is an optimum point of connection of an additional stream from HEN on a given overall heat exchanger area, in order to achieve maximum heat-flow rate, as well as the criteria for achieving that maximum. Novelty of the paper lays in that given criteria, needed to be fulfilled in order for the maximum amount of heat-flow rate to be exchanged for set heat exchanger operating conditions. Also, criteria equations are given, describing the conditions for which maximum heat-flow rate in such a heat exchanger in a HEN will not be reached. Derived dimensionless mathematical model is universal due to its coverage of all the operating regimes of the heat exchanger, different heat exchanger areas, overall heat transfer coefficients and also fluid streams of different kinds, mass-flow rates, specific heat capacities and temperatures.

Mathematical description of the problem

Elaboration of this mathematical model starts from the fact that a heat exchanger with given overall area, $A_{0\mathrm{tot}}$, is at disposal. While using mass-flow rate of streams A and B and their inlet temperatures from disposable HEN it is intended to change the heat-flow rate amount. Inlet parameters of the stream A and B are such that needed heat-flow rate would not be achieved by either of streams individually. Simultaneous performance of both streams necessary allows higher exchanged heat-flow rate then in a case when those streams perform individually. In order to achieve, along with the stream B, maximum heat-flow rate in such heat exchanger in a HEN, a point of stream A connection to a heat exchanger with a given overall area needs to be located. The amount of that maximum heat-flow rate needs to cover the amount of needed heat-flow rate. In other words, within this mathematical model a criterion for existing of the maximum heat-flow rate, as a local extremum, needs also to be obtained. Understanding the criterion of maximum heat-flow rate has a significant importance in design of new heat exchangers as well as in structural modifications of existing heat exchangers in actual facilities. It has been shown, when interventions in existing heat exchangers with given overall areas are undertaken, that, to achieve maximum heat-flow rate, there is a certain connection point for the additional stream. Exactly that point of connection of additional fluid stream determines the exchanging areas A and B. Criteria showing the existence of maximum heat-flow rate for different values of relevant parameters are derived and shown in following chapters.

Development of the maximum heat-flow rate criterion

In observed analysis overall counterflow heat exchanger area, $A_{0\mathrm{tot}}$, is given, thus also determining dimensionless value, $\pi_{2\mathrm{tot.}}$ According to fig. 1, entry temperatures of the weaker and stronger stream $T_1'_{\mathrm{B}}$ and T_2' are also known. Additionally, weaker stream with temperature $T_1'_{\mathrm{A}}$ is also at disposition, effecting area, $A_{0\mathrm{A}}$, aiming to achieve maximum heat-flow rate in that heat exchanger. Qualitative analysis of the problem already shows how, in a given case, an optimal heat exchanger area, A_{Aopt}, for which maximum heat-flow rate is achieved needs to exist.

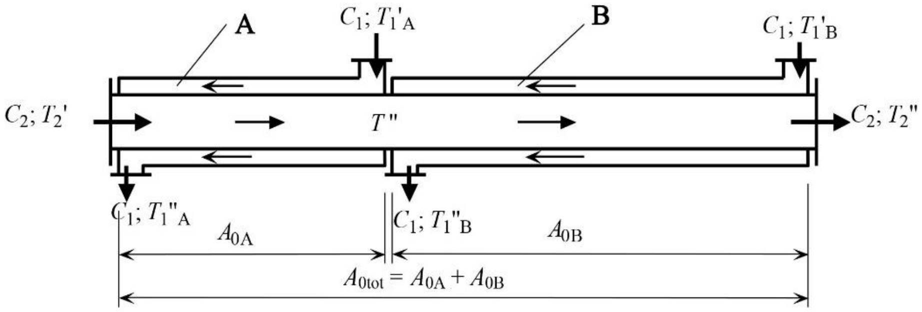

Figure 1. Along with explanation of the problem

With presumption that streams A and B, as weaker streams, have equal heat capacities, heat-flow rate can be expressed:

$$\Phi = C_1(T_{1A}^{'} - T_{1A}^{''} + T_{1B}^{'} - T_{1B}^{''}) \tag{1}$$

which is convenient to translate to a dimensionless form:

$$\frac{\Phi}{C_1(T_{1B}^{'} - T_2^{'})} = M\pi_{1A}(1 - \pi_3\pi_{1B}) + \pi_{1B} \tag{2}$$

In eq. (2) specific value is defined:

$$M = \frac{T_{1A}^{'} - T_2^{'}}{T_{1B}^{'} - T_2^{'}} \tag{3}$$

Value M is conveniently chosen because it represents ratio of difference between inlet temperatures of weaker stream A and stronger stream 2 to difference between inlet temperatures of the weaker stream B and stronger stream 2.

The following dimensionless expression is obtained:

$$\begin{gathered}\frac{\Phi}{C_1\left(T_{1B}^{'} - T_2^{'}\right)} = M\frac{1 - \exp\left[-(1-\pi_3)\pi_{2A}\right]}{1 - \pi_3\exp\left[-(1-\pi_3)\pi_{2A}\right]}\left\{1 - \pi_3\frac{1 - \exp\left[-(1-\pi_3)(\pi_{2tot} - \pi_{2A})\right]}{1 - \pi_3\exp\left[-(1-\pi_3)(\pi_{2tot} - \pi_{2A})\right]}\right\} + \\ + \frac{1 - \exp\left[-(1-\pi_3)(\pi_{2tot} - \pi_{2A})\right]}{1 - \pi_3\exp\left[-(1-\pi_3)(\pi_{2tot} - \pi_{2A})\right]}\end{gathered} \tag{4}$$

showing that observed heat-flow rate is a function of following dimensionless values: M, π_3, π_{2A}, and π_{2tot}, a function of four independent variables. Variable π_{2A} (= $k\,A_{0A}/C_1$) depends on value of the overall heat transfer coefficient, heat exchanger area, A, and heat capacity of the weaker streams A and B. As well as variable π_{2tot} (= $k\,A_{0tot}/C_1$) with difference in the overall heat exchanger area. Variable π_3 presents heat capacity ratio of weaker and stronger stream (= C_1/C_2).

Aim of this paper is obtaining the conditions for which function in eq. (4) achieves maximum as local extremum. This will be achieved when only value π_{2A} is varying within the interval $0 \le \pi_{2A} \le \pi_{2tot}$ and all other values are kept constant. However, explicit extrema conditions search is not possible, due to complexity of the function (4). That is why it is necessary to conduct an appropriate, also complex, numerical procedure. But, before obtaining that extremum, it is appropriate to list some of the specific values of the eq. (4):

For π_{2A} = 0.0 the following expression is gained:

$$\frac{\Phi}{C_1(T_{1B}^{'}-T_2^{'})}=\frac{1-\exp\left[-(1-\pi_3)\pi_{2tot}\right]}{1-\pi_3\exp\left[-(1-\pi_3)\pi_{2tot}\right]} \tag{5}$$

which does not depend on M so eq. (5) represents the solution for classic counterflow heat exchanger [29].

And for $\pi_{2A}=\pi_{2tot}$, eq. (4) transforms to following expression:

$$\frac{\Phi}{C_1(T_{1B}^{'}-T_2^{'})}=M\,\frac{1-\exp\left[-(1-\pi_3)\pi_{2tot}\right]}{1-\pi_3\exp\left[-(1-\pi_3)\pi_{2tot}\right]} \tag{6}$$

For given values M and π_{2tot}, maxima of eq. (4) can occur between values obtained when calculating eqs. (5) and (6). For M = 1.0, eqs. (5) and (6) evidently give the same values at the ends of the intervals π_{2A} = 0.0 and $\pi_{2A}=\pi_{2tot}$, which leads to conclusion that optimal value π_{2Aopt} in this case, regardless of $\pi_{3,}$ needs to be:

$$\pi_{2Aopt}=\frac{\pi_{2tot}}{2} \tag{7}$$

Specific cases of eq. (4)

As already emphasized before, explicit obtaining of eq. (4) extremum is practically impossible, which imposes the question of execution of such analysis for specific heat exchanger cases, reducing it to two cases: π_3 = 0.0 and π_3 = 1.0. The case π_3 = 0.0 is physically related to a situation when stronger stream evaporates or condenses. The other case, π_3 = 1.0 is related to a situation where both streams have equal heat capacities, therefore that case is often referred to as the balanced counterflow heat exchanger [29].

If π_3 = 0.0 is inserted into eq. (4), it is transformed to:

$$\frac{\Phi}{C_1(T_{1B}^{'}-T_2^{'})}=M\left[1-\exp(-\pi_{2A})\right]+1-\exp\left[-(\pi_{2tot}-\pi_{2A})\right] \tag{8}$$

It is interesting to examine whether the function (8) has a local extremum, with presumption that value π_{2tot} is a constant and value π_{2A} varies within the interval $0 \le \pi_{2A} \le \pi_{2tot}$. When deriving eq. (8) with respect to π_{2A} and equalizing it with zero, optimum value π_{2Aopt} is obtained, for which eq. (8) has a maximum:

$$\pi_{2Aopt}=\frac{1}{2}(\ln M+\pi_{2tot}) \tag{9}$$

By returning eq. (9) into eq. (8) it is easy to get to explicit expression for maximum heat-flow rate:

$$\left[\frac{\Phi}{C_1(T_{1B}^{'}-T_2^{'})}\right]_{max}=M+1-2\sqrt{M}\,\exp\left(-\frac{\pi_{2tot}}{2}\right) \tag{10}$$

Equations (9) and (10) show that for M > 0, eq. (8) has extremum (maximum). Meaning that with those conditions maximum possible heat-flow rate is transferred inside evaporator or condenser, which is the essential hypothesis of this paper. Optimum value $\pi_{2\mathrm{Aopt}}$ lies, depending on the M value, within interval $0 \le \pi_{2\mathrm{Aopt}} \le \pi_{2\mathrm{tot}}$. If $\pi_{2\mathrm{Aopt}}$ at the value of zero is wanted then from eq. (9) follows:

$$M = \exp(-\pi_{2\mathrm{tot}}) \tag{11}$$

with related maximum value:

$$\left[\frac{\Phi}{C_1(T_{1\mathrm{B}}^{'} - T_2^{'})}\right]_{\max,\ \pi_{2\mathrm{Aopt}}=0} = 1 - \exp(-\pi_{2\mathrm{tot}}) \tag{12}$$

If maximum at the end of the interval is wanted ($\pi_{2\mathrm{Aopt}} = \pi_{2\mathrm{tot}}$), then:

$$M = \exp(\pi_{2\mathrm{tot}}) \tag{13}$$

with related maximum:

$$\left[\frac{\Phi}{C_1(T_{1\mathrm{B}}^{'} - T_2^{'})}\right]_{\max,\ \pi_{2\mathrm{Aopt}}=\pi_{2\mathrm{tot}}} = \exp(\pi_{2\mathrm{tot}}) - 1 \tag{14}$$

From eq. (9), for M = 1.0, it is obvious that $\pi_{2\mathrm{Aopt}} = \pi_{2\mathrm{tot}}/2$, what is already confirmed with eq. (7).

For π_3 = 1.0 eq. (4) gives undefined form 0/0 so, using L'Hospital's rule, it is easy to transform it to a following form:

$$\frac{\Phi}{C_1(T_{1\mathrm{B}}^{'} - T_2^{'})} = M\,\frac{\pi_{2\mathrm{A}}}{\pi_{2\mathrm{A}}+1}\left(1 - \frac{\pi_{2\mathrm{tot}} - \pi_{2\mathrm{A}}}{\pi_{2\mathrm{tot}} - \pi_{2\mathrm{A}} + 1}\right) + \frac{\pi_{2\mathrm{tot}} - \pi_{2\mathrm{A}}}{\pi_{2\mathrm{tot}} - \pi_{2\mathrm{A}} + 1} \tag{15}$$

For M = 0.0 and $\pi_{2\mathrm{A}} = \pi_{2\mathrm{tot}}$, eq. (15) gives physically justified zero value. For $M > 0.0$ and $0 \le \pi_{2\mathrm{A}} \le \pi_{2\mathrm{tot}}$ it is necessary to examine if function in eq. (15) has a local extremum (maximum). Using extremum condition, expression for $\pi_{2\mathrm{Aopt}}$ arises:

$$\pi_{2\mathrm{Aopt}} = \frac{1 - \sqrt{-M(M\pi_{2\mathrm{tot}} + M - 2 - \pi_{2\mathrm{tot}})}}{M - 1} \tag{16}$$

Considering the fact that physically $M > 0.0$, then additional necessary condition follows from eq. (16), ensuring the fact that $\pi_{2\mathrm{Aopt}} \ge 0$:

$$M \le \frac{\pi_{2\mathrm{tot}} + 2}{\pi_{2\mathrm{tot}} + 1} \tag{17}$$

By inserting eq. (17) along with M = 1.0 into eq. (15) explicit expression for maximum heat-flow rate is obtained:

$$\left[\frac{\Phi}{C_1(T_{1\mathrm{B}}^{'} - T_2^{'})}\right]_{\max, M=1{,}0; \frac{\pi_{2\mathrm{tot}}}{2}} = \frac{\pi_{\mathrm{tot}}(\pi_{2\mathrm{tot}} + 4)}{(\pi_{2\mathrm{tot}} + 2)^2} \tag{18}$$

Connection of eqs. (11) and (17) produces the general condition which has to be fulfilled in order to achieve maximum heat-flow rate, which is at the same time a local extremum of the counterflow heat exchanger in heat exchanger network:

$$\exp(-\pi_{2\mathrm{tot}}) \le M \le \frac{\pi_{2\mathrm{tot}}+2}{\pi_{2\mathrm{tot}}+1} \tag{19}$$

Equations (11) and (13) also give the criteria for which local extremum (maximum) of the exchanged heat-flow rate will not occur:

$$0 < M < \exp(-\pi_{2\mathrm{tot}}) \tag{20}$$

$$M > \exp(\pi_{2\mathrm{tot}}) \tag{21}$$

If value M falls within the boundaries of the interval:

$$\frac{\pi_{2\mathrm{tot}}+2}{\pi_{2\mathrm{tot}}+1} \le M \le \exp(\pi_{2\mathrm{tot}}) \tag{22}$$

local extrema (maximum) of the heat-flow rate will be achieved only for certain values π_3 = const.

Within elaboration of the mathematical model in dimensionless form different values of physical parameters are possible, from which dimensionless numbers derived and applied in this paper are structured, like M, π_3, $\pi_{2\mathrm{A}}$, and $\pi_{2\mathrm{tot}}$. Those dimensionless numbers are defined by overall disposable heat exchanging area, area of heat exchangers A and B, overall heat transfer coefficient, heat capacities, mass-flow rates and temperatures of the fluid streams.

Diagrammatic representation and interpretation of the calculation results

Calculation results for the cases in which maximum heat-flow rate is achieved and for the cases in which maximum heat-flow rate is not achieved are given in this chapter. Results of the calculation are presented by adequate diagrams and then interpreted.

Cases in which maximum heat-flow rate is achieved

Case M = 0.5 and 1.0

Diagram on the left in fig. 2 shows that with stated conditions every parametric value π_3 = const. shows local extremum (maximum). For $\pi_{2\mathrm{A}} = 0.0$ heat-flow rate values are obtained for counterflow heat exchanger in which weaker stream is only stream B with inlet temperature $T_1'_{\mathrm{B}}$, while for the case $\pi_{2\mathrm{A}} = \pi_{2\mathrm{tot}}$ heat-flow rate values are obtained for the classic counterflow heat exchanger with weaker stream A and its inlet temperature $T_1'_{\mathrm{A}}$. Those values are determined by eqs. (5) and (6). It is evident that these values are lower than values of heat exchanger in HEN with the same inlet temperatures of both respective streams $T_1'_{\mathrm{A}}$ and $T_1'_{\mathrm{B}}$. That means for every π_3 = const. value of heat-flow rate with increase of $\pi_{2\mathrm{A}}$ firstly increases, achieves maximum in $\pi_{2\mathrm{Aopt}}$ and then continuously decreases with further increase of value $\pi_{2\mathrm{A}}$ to $\pi_{2\mathrm{tot}}$. Furthermore, it can be concluded that increase of maximum heat-flow rate is strongly emphasized for lower values of variable π_3, and that values of respective maxima decrease with the increase of variable π_3.

Diagram on the right in fig. 2 shows characteristic behavior of given results of the calculation, in the sense of symmetrical behavior of parameter value $\{\Phi/[C_1(T_1'_{\mathrm{A}} - T_2')]\}_{\max}$ for every parameter value π_3 = const., when value $M = 1.0$ is considered. As it is shown from the diagram, all those parametric curves achieve maximum for value $\pi_{2\mathrm{Aopt}} = \pi_{2\mathrm{tot}}/2 = 5.95/2 = 2.975$, and which are also confirmed by derived eq. (7) or directly eqs. (9) and (16) for

π_3 = 0.0 and π_3 = 1.0. Values of maximum dimensionless heat-flow rate decrease with the increase of value π_3. Also qualitative proof is laid out for the assertion that for M = 1.0 eqs. (5) and (6) give for individual value π_3 = const. identical values on the ends of the interval, *i. e.* for π_{2A} = 0.0 and $\pi_{2A} = \pi_{2Atot}$.

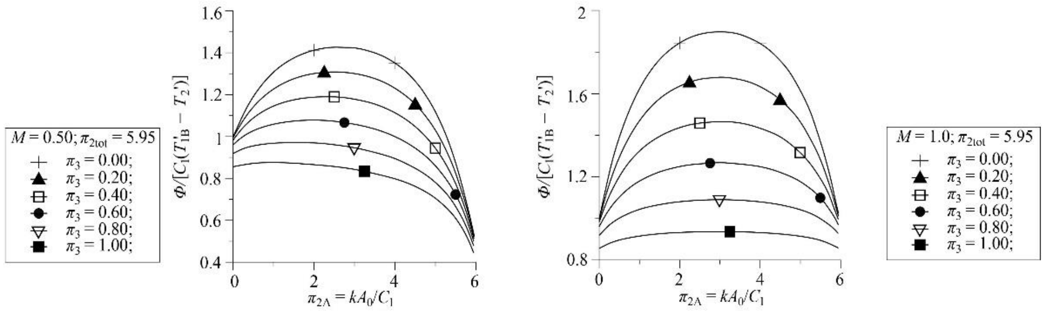

Figure 2. Dependence of dimensionless heat-flow rate on π_{2A} and π_3 with M = 0.5 and 1.0 and π_{2tot} = 5.95

Case M = 1.144

From eq. (19) it follows that M is in the interval $0.0026 \le M \le 1.144$ for examined case π_{2tot} = 5.95. It is observable that all of, up to this phase, analyzed cases conform to that criteria. If M = 1.144, then solution which conforms to the sought criteria is obtained, with the additional condition that for π_3 = 1.0 local extremum shows exactly on $\pi_{2Aopt} = \pi_{2tot}$ = 5.95. Diagram in fig. 3 shows every parametric value π_3 achieving local maxima. Diagram also shows that heat-flow rate decreases along with the increase of π_3 and that every parametric curve π_3 = const. achieves maximum as a local extremum, and for curve π_3 = 1.0 maximum is achieved on $\pi_{2Aopt} = \pi_{2tot}$.

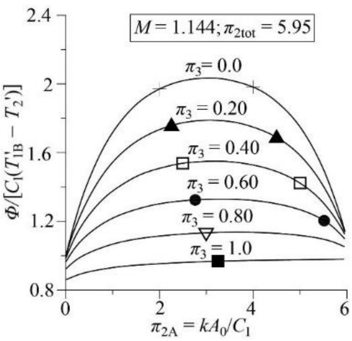

Figure 3. Dependence of dimensionless heat-flow rate on π_{2A} and π_3 with M = 1.144 and π_{2tot} = 5.95

Previous calculation has explicitly shown that if variable M lies within aforementioned interval, including the boundary values of that interval, that choice of specific fluid stream from available heat exchanger network can affect the increase of heat-flow rate. More than that, derived algorithm gives an answer to the positioning of the stream from HEN of given total area, with the goal of achieving maximum heat-flow rate.

Case M = 2.0

Further analysis includes the case where variable $M > [(\pi_{2tot} + 2)/(\pi_{2tot} + 1)]$, *i. e.*, when value of variable M is taken out of the criteria given by eq. (19), so therefore it is taken that $M = 2.0 > 1.144$. Diagram in fig. 4 shows interesting behavior of values $\Phi/[C_1(T_1{'}_A - T_2')]$ in dependence on π_{2A} and π_3 for chosen (constant) value π_{2tot}. Individual parametric curves π_3, with values within the interval $0 \le \pi_3 \le \pi_3^*$, show existence of maxima, while the remaining values π_3 do not show that behavior anymore. It is evident that in these cases ($\pi_3 \ge \pi_3^*$) continuous increasing of value $\Phi/[C_1(T_1{'}_A - T_2')]$ exists above entire field of value of variable π_{2A}. The highest values of heat-flow rate are obtained for π_{2tot} and those values are determined by eq. (6). In that case, value π_3^* actually represents the value of variable

π_3 for which it is $\pi_{2\text{Aopt}} = \pi_{2\text{tot}}$. Due to complexity of eq. (4) it is not explicitly possible to find π_3^*, problem is rather solved by the adequate numerical procedure. By that procedure it is obtained that $\pi_3^* = 0.5$, so that diagram in fig. 4 shows values $\pi_{2\text{Aopt}}$ with associated $\{\Phi/[C_1(T_1'{}_\text{A} - T_2')]\}_\text{max}$ for exactly that existing interval of variable π_3, $0 \le \pi_3 \le \pi_3^* = 0.5$.

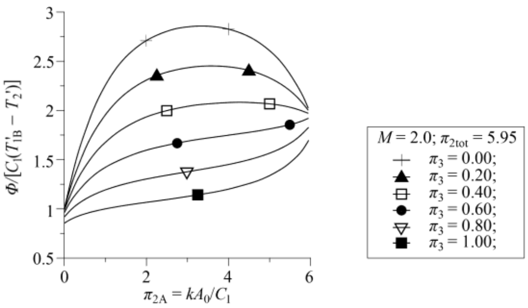

Figure 4. Dependence of dimensionless heat-flow rate on $\pi_{2\text{A}}$ and π_3 with $M = 2.0$ and $\pi_{2\text{tot}} = 5.95$

Cases in which maximum heat-flow rate is not achieved

If value M has a value given through criteria in eqs. (20) and (21), then there is no value $\pi_{2\text{Aopt}}$ for observed heat exchanger in HEN, for which a possibility of achieving maximum heat-flow given as local extremum would appear. Concerning proposition is quantified for value $\pi_{2\text{tot}} = 1.0$.

Case $M < \exp(-\pi_{2tot})$ and $M > \exp(\pi_{2tot})$

According to eq. (20), boundary case for value of variable M is $M = \exp(-\pi_{2\text{tot}}) = \exp(-1) = 0.3679$ so case in which $M = 0.3 < 0.3679$ is chosen. For observed case, diagram on the left in fig. 5 shows dimensionless heat-flow rate depending on variable $\pi_{2\text{A}}$ and variable π_3. From the diagram it is obvious how value of dimensionless heat-flow rate is continually decreasing for every $\pi_3 = \text{const.}$, with increase of variable $\pi_{2\text{A}}$ from $\pi_{2\text{A}} = 0.0$ to $\pi_{2\text{A}} = \pi_{2\text{tot}} = 1.0$. Furthermore, value of dimensionless heat-flow rate increases with the decrease of π_3. Expected fact is evident absence of maximum as local extremum. Maximum heat-flow rate values, for a particular $\pi_3 = \text{const.}$ are obtained when $\pi_{2\text{A}} = 0.0$, and minimum values for $\pi_{2\text{A}} = \pi_{2\text{tot}} = 1.0$.

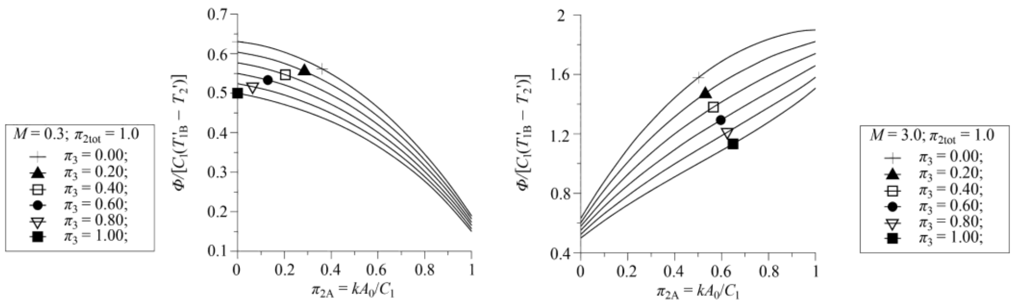

Figure 5. Dependence of dimensionless heat-flow rate on $\pi_{2\text{A}}$ and π_3 with $M = 0.3$ and 3.0 and $\pi_{2\text{tot}} = 1.0$

According to criterion in eq. (21) follows that the value of M must be $M > \exp(1) = 2.718$. Therefore, in further calculation it is taken that $M = 3.0$. Diagram on the right in fig. 5 shows that in this case dimensionless heat-flow rate, when $\pi_3 = \text{const.}$, continually increases with the increase of $\pi_{2\text{A}}$, thus differing from previous case when it was decreasing. In addition, it is obvious that those values decrease with the increase of value π_3. It is important to notice that maximum as a local extremum has not been reached in any case, what is quantified by criterion given in eq. (21).

Summarized results of calculation

Summarized results of calculation are provided with two tables. Table 1 presents the cases in which maximum heat-flow rate is achieved for $\pi_{2tot} = 5.95$ and when π_3 varies between 0.0 and 1.0. A special case is also given, where maximum heat-flow rate is achieved below value $\pi_3^* = 0.5$ for $M = 2.0$. Table 2 presents the cases in which maximum heat-flow rate is not achieved for $\pi_{2tot} = 1.0$ and in which π_3 varies between 0.0 and 1.0.

Table 1. Results for π_{2tot} = 5.95 and π_3 = 0.0, 0.2, 0.4, 0.6, 0.8, 1.0

Maximum heat-flow rate is achieved $0.0026 \le M \le 1.144$	Below value π_3^* = 0.5 maximum heat-flow rate is achieved $1.144 \le M \le 383.8$
M = 0.5	M = 2.0
M = 1.0	
M = 1.114	

Table 2. Cases in which maximum heat-flow rate is not achieved for π_{2tot} = 1.0 and π_3 = 0.0, 0.2, 0.4, 0.6, 0.8, 1.0

Maximum heat-flow rate is not achieved for all π_3 values		
π_{2tot} = 1.0	M < 0.3679 M = 0.3	M > 2.718 M = 3.0

Case study: TPP Plomin, Unit 2

In order to understand the presented methodology and its application, a case study of a condenser in the Thermal Power Plant (TPP) Plomin, Unit 2 is given as an example.

Relevant data describing operation of condenser are given:
– mass-flow rate of condensing steam – q_{ms} = 116.36 kg/s,
– steam pressure – p = 0.041 bar,
– saturation temperature – T_2' = 302.15 K,
– dryness fraction at the inlet of condenser – x = 0.90,
– overall heat exchanger area – A_{0tot} = 10,516 m^2,
– sea cooling water temperature at the inlet of condenser – $T_1{'}_A$ = 293.15 K, and
– sea cooling water temperature at the outlet of condenser – $T_1{''}_A$ = 300.65 K.

This example corresponds to a case π_3 = 0.0 since the steam condenses totally. Cooling water inlet temperature is $T_1{'}_A$ = $T_1{'}_B$ = 293.15 K, so, according to eq. (3), M = 1.0. Temperature profile of the cooling water and condensing steam in a given heat exchanger is shown in fig. 6.

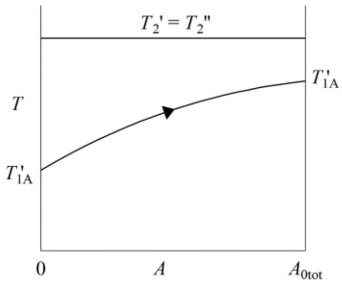

Figure 6. Qualitative display of stream temperatures in a condenser

According to given data logarithmic mean temperature difference between streams is:

$$\Delta T_{m,\log} = \frac{(T_2' - T_{1A}') - (T_2' - T_{1A}'')}{\ln \dfrac{T_2' - T_{1A}'}{T_2' - T_{1A}''}} = 4.1858 \text{ K} \tag{23}$$

Achieved heat-flow rate in a condenser is:

$$\Phi = q_{ms} x r (0.041 \text{ bar}) = \\ = 116.36 \times 0.91 \times 2{,}432.31 = 257551.5 \text{ kW} \tag{24}$$

and heat capacity of the weaker stream (cooling water stream) is:

$$C_1 = \frac{\Phi}{T_{1A}^{''} - T_{1A}^{'}} = \frac{257551.5}{300.65 - 293.15} = 34340.2 \text{ kW/K} \tag{25}$$

Given equation:

$$\Phi = kA_{0\text{tot}} \Delta T_{\text{m,log}} \tag{26}$$

results with $kA_{0\text{tot}}$

$$kA_{0\text{tot}} = \frac{\Phi}{\Delta T_{\text{m,log}}} = \frac{257551.5}{4.1858} = 61529.82 \text{ kW/K} \tag{27}$$

and therefore

$$\pi_{2\text{tot}} = \frac{kA_{0\text{tot}}}{C_1} = \frac{61529.82}{34340.2} = 1.792 \tag{28}$$

Optimum value $\pi_{2\text{Aopt}}$ from eq. (7) is:

$$\pi_{2\text{Aopt}} = \frac{\pi_{2\text{tot}}}{2} = \frac{1.792}{2} = 0.896 \tag{29}$$

and according to eq. (10) value of parameter $\{\Phi/[C_1(T_1{'}_{\text{B}} - T_2{'})]\}_{\max}$ is:

$$\left[\frac{\Phi}{C_1(T_{1A}^{'} - T_2^{'})}\right]_{\max} = M + 1 - 2\sqrt{M}\exp\left(-\pi_{2\text{Aopt}}\right) = 1 + 1 - 2\exp(-0.896) = 1.184 \tag{30}$$

So maximum heat-flow rate is as follows:

$$\Phi_{\max} = 1.184\, C_1(T_2^{'} - T_{1A}^{'}) = 1.184 \times 34340.2 \times (302.15 - 293.15) = 365929.2 \text{ kW} \tag{31}$$

Ratio between maximum heat-flow rate and achieved heat-flow rate in a condenser is:

$$\omega_{\text{A}} = \omega_{\text{B}} = \frac{\Phi_{\max}}{\Phi} = \frac{365929.2}{257551.5} = 1.42 \tag{32}$$

The result $\omega_{\text{A}} = \omega_{\text{B}} = 1.42$ shows how this type of condenser operation can achieve 42% more heat-flow rate in a condenser. This means that for the same condenser inlet steam state and for the same condenser outlet steam state 42% more steam can be condensed. Evidently, this type of condenser operation can increase overall steam mass-flow rate in a facility. Thus, with the same thermal efficiency, 42% greater turbine power is gained. Of course, this type of condenser operation demands design modifications. It is also necessary to note that for such condenser operation double mass-flow rate of the cooling water should be at disposal.

Conclusions

In this paper the mathematical model in dimensionless form has been developed, describing operation of a heat exchanger in a HEN, with given overall area, based on the heat-flow rate criterion. Under the presumption of heat exchanger being a part of the HEN, solution for the given task rests in a possibility of connecting an additional fluid stream to a certain point of observed heat exchanger from an existing HEN. The connection point on an observed heat exchanger needs to allow the maximum exchanged heat-flow rate. The maximum heat-flow rate existence criteria were derived using different relevant dimensionless variables defined by overall heat exchanger area, heat exchanger area A and B, overall heat transfer coefficient and temperature, mass-flow rates and heat capacities of the fluid streams. General criterion which needs to be fulfilled in order for the maximum heat-flow rate of the counterflow heat exchanger in a HEN to be achieved is derived, as well as the criteria for which maximum heat-flow rate will not be achieved. The criterion for achieving maximum heat-flow rate for certain values of parameter π_3 is also given. Results of the calculations are presented by adequate diagrams and then interpreted. For given values of dimensionless variables cases fulfilling and also those not fulfilling the criterion of the maximum heat-flow have been presented and discussed.

A case study of a condenser in the TPP Plomin, Unit 2 is given as an example of derived mathematical model application. Maximum heat-flow rate exchanged in a condenser, calculated using presented methodology, is 42% higher than actually achieved heat-flow rate in a condenser.

Finding the criteria which include various operating regimes of the counterflow heat exchangers in complex HEN shows the possibility of achieving or not achieving maximum heat-flow rate in a chosen heat exchanger. Maximum heat-flow rate, which is higher than the heat-flow rate achieved separately either by heat exchanger A or by heat exchanger B, can be significant in peak heat loads in heat exchanger operation. Thereby this paper advances the present state of knowledge in the analysis of HEN.

Nomenclature

A_{0A} – heat exchanger area A, [m^2]
A_{0B} – heat exchanger area B, [m^2]
A_{0tot} – overall heat exchanger area, [m^2]
A_{Aop}t – optimal heat exchanger area, [m^2]
C_1 – heat capacity of weaker streams A and B, [WK^{-1}]
C_2 – heat capacity of stronger stream, [WK^{-1}]
k – overall heat transfer coefficient, [Wm^{-2}K^{-1}]
$T_1{}'_A$ – inlet temperature of weaker stream A, [K]
$T_1{}''_A$ – outlet temperature of weaker stream A, [K]
$T_1{}'_B$ – inlet temperature of weaker stream B, [K]
$T_1{}''_B$ – outlet temperature of weaker stream B, [K]
$T_2{}'$ – inlet temperature of stronger stream, [K]
T'' – temperature of stronger stream at the connection point of additional stream, [K]
$T_2{}''$ – outlet temperature of stronger stream, [K]

Greek symbols

π_{1A} – effectiveness of the heat exchanger A (= ε_A), [–]
π_{1B} – effectiveness of the heat exchanger B (= ε_B), [–]
π_{2tot} – number of transfer units for entire heat exchanger (= $k\,A_{0tot}/C_1$), [–]
π_3 – dimensionless number presenting heat capacity ratio (= C_1/C_2), [–]
π_{2Aopt} – dimensionless number presenting optimal connection point of another stream to heat exchanger area in order to obtain maximum heat-flow rate, [–]
π_{2A} – number of transfer units for heat exchanger A (= $k\,A_{0A}/C_1$), [–]
$\Phi/[C_1(T_1{}'_B - T_2{}')]$ – dimensionless heat-flow rate, [–]
Φ – heat-flow rate, [W]

References

[1] Novak Pintarič, Z., Kravanja, Z., A Methodology for the Synthesis of Heat Exchanger Networks Having Large Numbers of Uncertain Parameters, *Energy, 92* (2015), Part 3, pp. 373-382
[2] Wang, Z., *et al.*, A Novel Optimization Framework for Designing Multi-Stream Compact Heat Exchangers and Associated Network, *Applied Thermal Engineering, 16* (2017), Apr., pp. 110-125
[3] Floudas, C. A., *et al*., Automatic Synthesis of Optimum Heat Exchanger Network Configurations, *AIChE Journal, 32* (1986), 2, pp. 276-290
[4] Zhang, B. J., *et al.*, Simultaneous Design of Heat Exchanger Network for Heat Integration using Hot Direct Discharges/Feeds between Process Plants, *Energy, 109* (2016), Aug., pp. 400-411

[5] Escobar, M., Trierweiler, J. O., Optimal Heat Exchanger Network Synthesis: A Case Study Comparison, *Applied Thermal Engineering, 51* (2013), 1-2, pp. 801-826
[6] Alwi, S. R. W., *et al*., A Process Integration Targeting Method for Hybrid Power Systems, *Energy, 44* (2012), 1, pp. 6-10
[7] Tan, R. R., Foo, D. C. Y., Pinch Analysis Approach to Carbon-constrained Energy Sector Planning, *Energy, 32* (2007), 8, pp. 1422-1429
[8] Manan, Z. A., *et al.*, Generic Carbon Cascade Analysis Technique for Carbon Emission Management, *Applied Thermal Engineering, 70* (2014), 2, pp. 1141-1147
[9] Ooi, R. E. H., *et al*., Carbon Constrained Energy Planning (CCEP) for Sustainable Power Generation Sector with Automated Targeting Model, *Industrial & Engineering Chemistry Research, 52* (2013), 29, pp. 9889-9896
[10] Picon-Nunez, M., Application of Process Integration Techniques for the Efficient Use of Energy in a Urea Fertiliser Plant: A Case Study, in: *Handbook of Process Integration* (Ed. J. J. Klemes), Woodhead Publishing, Sawston, UK, 2013, pp. 914-937
[11] Smith, R., *et al*., Recent Development in the Retrofit of Heat Exchanger Networks, *Applied Thermal Engineering, 30* (2010), 16, pp. 2281-2289
[12] Pan, M., *et al*., A Novel Optimization Approach of Improving Energy Recovery in Retrofitting Heat Exchanger Network with Exchanger Details, *Energy, 57* (2013), Aug., pp. 188-200
[13] Zheng, K., *et al*., A Method for Flexible Heat Exchanger Network Design Under Severe Operation Uncertainty, *Chemical Engineering & Technology, 36* (2013), 5, pp. 757-765
[14] Boonsup, C., Siemanond, K., Heat Exchanger Network Design with Multi-stream Exchangers Using Stage-wise Superstructure, *Computer Aided Chemical Engineering, 38* (2016), pp. 1869-1874
[15] Watson, A. J. H., *et al*., Multistream Heat Exchanger Modeling and Design, *American Institute of Chemical Engineers Journal, 61* (2015), 10, pp. 3390-3403
[16] Guo, K., *et al*., Design Optimization of Multi-stream Plate Fin Heat Exchangers with Multiple Fin Types, *Applied Thermal Engineering, 131* (2018), Feb., pp. 30-40
[17] Li, J., *et al*., Synthesis of Large-scale Multi-stream Heat Exchanger Networks Using a Stepwise Optimization Method, *Journal of the Taiwan Institute of Chemical Engineers, 45* (2014), 2, pp. 508-517
[18] Xiangkun, M., *et al*., Synthesis of Multi-stream Heat Exchanger Network for Multi-period Operation with Genetic/simulated Annealing Algorithms, *Applied Thermal Eng., 28* (2008), 8-9, pp. 809-823
[19] Yuan, D., *et al*., An Automated Method for Synthesizing a Multi-stream Heat Exchanger Network Based on Stream Pseudo-temperature, *Computer Aided Chemical Eng., 21* (2006), Dec., pp. 919-924
[20] Zhang, H., *et al*., A Novel Simultaneous Optimization Model with Efficient Stream Arrangement for Heat Exchanger Network Synthesis, *Applied Thermal Engineering, 110* (2017), Jan., pp. 1659-1673
[21] Teng, W. S., *et al*., Revisiting Adsorption Cooling Cycle from Mathematical Modeling to System Development, *Renewable and Sustainable Energy Reviews, 63* (2016), Sept., pp. 315-332
[22] Wang, H., *et al*., Optimum Performance of a Double Absorption Heat Transformer, *Energy Conversion and Management, 122* (2016), Aug., pp. 350-356
[23] Ochoa, A. A. V., *et al*., Dynamic Study of a Single Effect Absorption Chiller Using the Pair LiBr/H2O, *Energy Conversion and Management, 108* (2016), Jan., pp. 30-42
[24] He, W. F., *et al*., Performance Analysis of an Air-heated Humidification-dehumidification Desalination Plant Powered by Low Grade Waste Heat, *Energy Conversion and Manag., 118* (2016), June, pp. 12-20
[25] Wang, J., *et al*., Thermodynamic Analysis of a New Combined Cooling and Power System Using Ammonia-water Mixture, *Energy Conversion and Management, 117* (2016), June, pp. 335-342
[26] Cui, X., *et al*., Performance Evaluation of an Indirect Pre-cooling Evaporative Heat Exchanger Operating in Hot and Humid Climate, *Energy Conversion and Manag., 102* (2015), Sept., pp. 140-150
[27] Taler, D., Mathematical Modeling and Control of Plate Fin and Tube Heat Exchangers, *Energy Conversion and Management, 96* (2015), May, pp. 452-462
[28] Ma, H., *et al*., Assessment of the Optimum Operation Conditions on a Heat Pipe Heat Exchanger for Waste Heat Recovery in Steel Industry, *Renewable and Sustainable Energy Reviews, 79* (2017), Nov., pp. 50-60
[29] Bejan, A., *Advanced Engineering Thermodynamics*, John Wiley and Sons Inc., New York, USA, 1988

Paper submitted: December 31, 2017
Paper revised: March 3, 2018
Paper accepted: March 9, 2018